RESEARCH

A mathematical model for evaluating the impact of nonpharmaceutical interventions on the early COVID-19 epidemic in the United Kingdom

Hongyu Zhang[1][*] and Shuanglin Jing[2]

[*]Correspondence:
zhanghongyu9100@163.com
[1]College of Mathematical Sciences,
Mudanjiang Normal University,
Mudanjiang, Heilongjiang, 157011,
China
Full list of author information is
available at the end of the article

Abstract

The coronavirus disease 2019 (COVID-19) presents a severe and urgent threat to global health. In response to the COVID-19 pandemic, many countries have implemented nonpharmaceutical interventions (NPIs), including national workplace and school closures, personal protection, social distancing, contact tracing, testing, home quarantine, and isolation. To evaluate the effectiveness of these NPIs in mitigating the spread of early COVID-19 and predict the epidemic trend in the United Kingdom, we developed a compartmental model to mimic the transmission with time-varying transmission rate, contact rate, disease-induced mortality rate, proportion of quarantined close contacts, and hospitalization rate. The model was fitted to the number of confirmed new cases and daily number of deaths in five stages with a Markov Chain Monte Carlo method. We quantified the effectiveness of NPIs and found that if the transmission rate, contact rate, and hospitalization rate were approximately equal to those in the second stage of the most strict NPIs, and the proportion of quarantined close contacts increased by 3%, then the epidemic would die out as early as January 12, 2021, with around 1,533,000 final cumulative number of confirmed cases, and around 55,610 final cumulative number of deaths.

Keywords: COVID-19; Reproduction number; Markov Chain Monte Carlo; Nonpharmaceutical interventions; Predictions

1 Introduction

Severe acute respiratory syndrome coronavirus 2 (SARS-CoV-2) emerged in December 2019 and caused numerous COVID-19 outbreaks worldwide [1]. Neither a vaccine against the virus nor a specific treatment was available at that moment [2]. Infected individuals may develop some typical symptoms, including fever, continuous cough, fatigue, headache, and sore throat. More than 50% of the severe cases may die of the infection [3], while some exposed and asymptomatic infectious people are also contagious [4], which complicates the efforts to control the pandemic through intervention strategies [5].

Effective surveillance and early detection of SARS-CoV-2 transmission in unaffected regions are essential to mitigate the initial spread of the infection and substantially reduce

health care, economic, and societal burden [6]. The findings of the Global Health Security Index [7] show that only 19% of countries can detect and report epidemics of potential international concerns rapidly, and less than 5% of countries can respond to and mitigate the spread of an epidemic promptly. Hence, almost no countries are fully prepared for epidemics or pandemics [8]. The National Health System (NHS) of the United Kingdom (UK) has evolved as one of the largest healthcare systems in the world, which is based on need instead of an individual's ability to pay for the treatment [9]. However, the UK was one of the most affected countries by COVID-19 in the world.

The UK medical community suggested that the government should have followed the early recommendation of the World Health Organization (WHO) based on responses to past epidemics, including SARS in 2003, MERS in 2012, and H1N1 [10]. The UK did not initiate a massive testing program for COVID-19 suspected patients and provide appropriate personal protective equipment (PPE) and pharmaceutical resources for healthcare workers [11]. Thus, coping with this emerging infectious disease and its uncontrollable worldwide expansion has become a great challenge. The mitigating efforts during the early COVID-19 outbreak from January 31 to November 5, 2020 in the UK could be analyzed in five stages. The first stage was from January 31, 2020, when the first two confirmed cases were reported by the UK and hospitalized, till March 23, 2020, when the UK implemented a national lockdown. The second stage was from March 23 to May 13, 2020, when the UK ended the national lockdown. The third stage was from May 13 to July 4, 2020, during which the UK gradually reopened. The fourth stage was from July 4 to September 24, 2020, during which the UK returned to normal life. The fifth stage was from September 24 to November 5, 2020, during which the UK intensified the NPIs due to the second outbreak.

The effectiveness of these interventions can be quantified by an effective reproduction number $R_e(t)$, which represents the average number of infections produced by an infected individual during the variable infectious period [12]. If $R_e(t) < 1$, the epidemic will die out, otherwise, the number of new infections keeps increasing until the epidemic peaks when $R_e(t) = 1$. The effective reproduction number is a function of three factors, namely, the fraction of the population that is immune to the infection, the number of contacts between individuals after implementing NPIs or using PPE, and the length of time during which an infectious person is spreading the virus. Because the fraction of people who were immune to COVID-19 infection in the UK was still tiny, the epidemic did not stop because of herd immunity. People reduced their number of contacts and used PPE to prevent the infection. The improvement of detection efficiency could shorten the transmission time of SARS-CoV-2 [13]. These strategies were implemented together to bring $R_e(t)$ below 1 and flatten the epidemic curve. Thus, the trend of the epidemic growth across the UK was no longer exponential since the strengthening of the NPIs [13].

Mathematical models play a crucial role in epidemiology for understanding and predicting the spread of infectious diseases. Two commonly used approaches are modeling using differential equations and modeling using agent-based network models. In the case of differential equations, these models describe the interactions between different compartments of a population (e.g., susceptible, infected, recovered) using differential equations [14–16]. They are often used to capture the average behavior of a population and provide insights into the dynamics of disease transmission. On the other hand, agent-based network models simulate the interactions between individual agents in a population, allow-

ing for a more detailed representation of heterogeneities and network structures [17–19]. These models capture the behavior and movement patterns of individuals and can provide insights into the impact of individual-level factors on disease spread. We developed a system of ordinary differential equations (ODEs) to study the transmission dynamics of COVID-19 in the UK. The uncertainty in the model parameters can lead to significant inaccuracy in model projections [20]. We used a Markov Chain Monte Carlo (MCMC) method to estimate the mean values of these parameters and quantify this uncertainty [21]. We applied the Delayed Rejection Adaptive Metropolis (DRAM) algorithm to ensure the accuracy of parameter estimations [22].

We fitted the model with the daily number of confirmed new cases and daily number of deaths in the five stages from January 31 to November 5, 2020. We drove the effective reproduction numbers for the five stages. We used the partial rank correlation coefficient (PRCC) for the global sensitivity analysis. The model predicted the future trends of the epidemic and evaluated the effectiveness of NPIs under different scenarios.

2 The mathematical model

Based on the clinical progress of COVID-19, the epidemiological characteristics, and the countermeasures in the UK, we developed a compartmental model where individuals are divided into susceptible (S), exposed (E), symptomatic infectious (I), asymptomatic infectious (A), hospitalized (H), recovered (R), dead (D), quarantined susceptible (S_q), and quarantined exposed (E_q) compartments.

The schematic diagram for the model is illustrated in Figure 1, and the model parameters as well as initial values are shown in Tables 1 and 2. Let the transmission probability be $\beta(t)$ and the contact rate be $c(t)$. The susceptible individuals can be infected by E, A, or I. A proportion, $q(t)$, of individuals exposed to the infection is quarantined through contact tracing. The quarantined individuals can move to the state S_q or E_q at the rate $(1 - \beta(t))c(t)q(t)$ or $\beta(t)c(t)q(t)$, depending on whether they are effectively infected. The parameter λ is the release rate of quarantined uninfected contacts, and $\delta_q(t)$ is the rate at which quarantined infected individuals are hospitalized. The proportion, $1 - q(t)$, of individuals exposed to the infection who are missed from the contact tracing and enter the exposed state, E, at the rate $\beta(t)c(t)(1 - q(t))$. The fraction ρ of exposed individuals progresses to the symptomatic infectious state I at the rate $\rho\alpha$, while the rest of the ex-
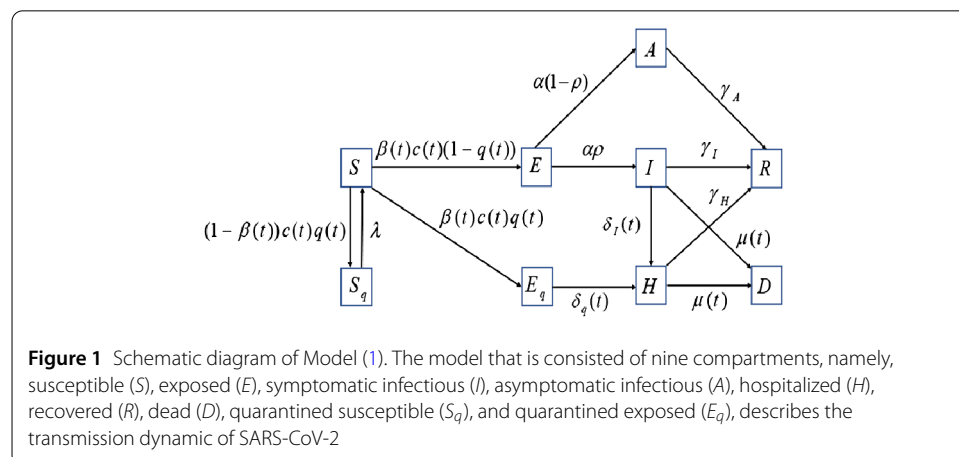

Figure 1 Schematic diagram of Model (1). The model that is consisted of nine compartments, namely, susceptible (*S*), exposed (*E*), symptomatic infectious (*I*), asymptomatic infectious (*A*), hospitalized (*H*), recovered (*R*), dead (*D*), quarantined susceptible (*S_q*), and quarantined exposed (*E_q*), describes the transmission dynamic of SARS-CoV-2

Table 1 Parameters of Model (1)

Parameter	Description	Unit	Estimated mean value	Std	95% CI	Source
$\beta(t)$	The transmission probability	Dimensionless	0.0293	0.0016	[0.0262, 0.0324]	MCMC
			0.0197	0.0010	[0.0177, 0.0217]	
			0.0037	0.0008	[0.0021, 0.0053]	
			0.0427	0.0025	[0.0378, 0.0476]	
			0.0659	0.0082	[0.0498, 0.0820]	
$c(t)$	The contact rate	1/Day	13.8780	0.6569	[12.5905, 15.1655]	MCMC
			5.6702	0.2203	[5.2384, 6.1020]	
			9.2718	0.5021	[8.2877, 10.2559]	
			10.9740	0.5102	[9.9740, 11.9740]	
			11.3180	0.5625	[10.2155, 12.4205]	
α	The incubation rate of exposed individuals	1/Day	1/5	–	–	[23]
ρ	The fraction of symptomatic infectious individuals	Dimensionless	0.6	–	–	[24]
γ_I	The recovery rate of symptomatic infectious individuals	1/Day	1/12	–	–	[25]
γ_H	The recovery rate of hospitalized individuals	1/Day	1/10	–	–	[26]
γ_A	The recovery rate of asymptomatic infectious individuals	1/Day	1/9.5	–	–	[27]
$\delta_I(t)$	The rate at which symptomatic infectious individuals are hospitalized	1/Day	0.0432	0.0131	[0.0175, 0.0689]	MCMC
			0.0536	6.59×10^{-3}	[0.0407, 0.0665]	
			0.0379	7.16×10^{-3}	[0.0237, 0.0521]	
			0.1823	8.38×10^{-3}	[0.1659, 0.1987]	
			0.0309	0.0139	[0.0037, 0.0581]	
$\mu(t)$	The disease-induced mortality rate	1/Day	7.23×10^{-4}	2.00×10^{-4}	$[3.32 \times 10^{-4}, 1.11 \times 10^{-3}]$	MCMC
			5.53×10^{-3}	5.40×10^{-4}	$[4.48 \times 10^{-3}, 6.59 \times 10^{-3}]$	
			3.05×10^{-3}	2.18×10^{-4}	$[2.62 \times 10^{-3}, 3.47 \times 10^{-3}]$	
			7.66×10^{-4}	1.50×10^{-4}	$[4.71 \times 10^{-4}, 1.06 \times 10^{-3}]$	
			1.12×10^{-3}	1.17×10^{-4}	$[8.86 \times 10^{-4}, 1.34 \times 10^{-3}]$	
θ	The factor for reduced transmission rate in asymptomatic infectious individuals	Dimensionless	0.5	–	–	[28]
ν	The factor for reduced transmission rate among exposed individuals	Dimensionless	0.5	–	–	[29]
$q(t)$	The proportion of quarantined close contacts	Dimensionless	0	–	–	Assume
			0	–	–	
			0.8517	0.0628	[0.7286, 0.9748]	MCMC
			0.5178	0.0280	[0.4629, 0.5727]	
			0.8231	0.0243	[0.7755, 0.8707]	
λ	The release rate of the quarantined uninfected lose contacts	1/Day	1/14	–	–	[30]
$\delta_q(t)$	The rate at which quarantined infected individuals are hospitalized	1/Day	0	–	–	Assume
			0	–	–	
			0.0574	0.0071	[0.0435, 0.0713]	MCMC
			0.1738	0.0198	[0.1350, 0.2126]	
			0.1186	0.0136	[0.0919, 0.1453]	

Table 2 Initial values of Model (1)

Initial value	Description	Unit	Estimated	Std	95%CI	Source
$S(0)$	The initial size of susceptible population	Number	66,573,504	–	–	[31]
$E(0)$	The initial size of	Number	11.3230	1.1634	[9.0427, 13.6033]	MCMC
$I(0)$	The initial size of symptomatic infectious population	Number	4.1686	0.3280	[3.5257, 4.8115]	MCMC
$A(0)$	The initial size of asymptomatic infectious population	Number	1.4524	0.3050	[0.8546, 2.0502]	MCMC
$S_q(0)$	The initial size of quarantined susceptible population	Number	0	–	–	Assume
$E_q(0)$	The initial size of quarantined exposed population	Number	0	–	–	Assume
$H(0)$	The initial number of hospitalized individuals	Number	2	–	–	[2]
$R(0)$	The initial number of recovered individuals	Number	0	–	–	[2]
$D(0)$	The initial number of dead individuals	Number	0	–	–	[2]

posed individuals enter the asymptomatic infectious state, A, at the rate $(1 - \rho)\alpha$. The asymptomatic infectious individuals recover at the rate γ_A. The symptomatic infectious individuals are hospitalized at the rate $\delta_I(t)$ and recover at the rate γ_H, or die at the rate $\mu(t)$. The resulting system of ODEs is

$$
\begin{cases}
S'(t) = -[\beta(t)c(t) + c(t)q(t)(1 - \beta(t))]\frac{S}{N}(\nu E + \theta A + I) + \lambda S_q, \\
E'(t) = \beta(t)c(t)(1 - q(t))\frac{S}{N}(\nu E + \theta A + I) - \alpha E, \\
I'(t) = \rho\alpha E - (\gamma_I + \delta_I(t) + \mu(t))I, \\
A'(t) = (1 - \rho)\alpha E - \gamma_A A, \\
S'_q(t) = c(t)q(t)(1 - \beta(t))\frac{S}{N}(\nu E + \theta A + I) - \lambda S_q, \\
E'_q(t) = c(t)q(t)\beta(t)\frac{S}{N}(\nu E + \theta A + I) - \delta_q(t)E_q, \\
H'(t) = \delta_I(t)I + \delta_q(t)E_q - (\gamma_H + \mu(t))H, \\
R'(t) = \gamma_I I + \gamma_A A + \gamma_H H, \\
D'(t) = \mu(t)(I + H).
\end{cases}
\tag{1}
$$

The total number of individuals is

$$
N(t) = S(t) + E(t) + I(t) + A(t) + S_q(t) + E_q(t) + H(t) + R(t) + D(t).
$$

We assume that the transmission rate, $\beta(t)$, the contact rate, $c(t)$, the disease-induced mortality rate, $\mu(t)$, the rate at which symptomatic infectious individuals are hospitalized, $\delta_I(t)$, the quarantined proportion of close contacts, $q(t)$, and the rate at which quarantined infected individuals are hospitalized, $\delta_q(t)$, all vary with time t. These time-dependent parameters reflect the effect of varying NPIs over the five stages.

3 Parameter estimation and data fitting

The cumulative number of confirmed cases, the total number of deaths, the daily number of confirmed new cases, and the daily number of deaths were obtained from the official UK Government website [2].

We assumed $S(0)$ = 66,573,504, which was the total population of the UK [31]. On January 31, 2020, as the first two confirmed cases were reported by the UK and hospitalized, we assumed $H(0)$ = 2, and January 31, 2020, was the start date. At this time, no one was recovered, quarantined, or dead, $R(0) = S_q(0) = E_q(0) = D(0) = 0$. The parameters used in the simulations were α = 1/5 [23], ρ = 0.6 [24], γ_I = 1/12 [25], γ_H = 1/10 [26], γ_A = 1/9.5 [27], $\nu = \theta = 0.5$ [28, 29], and λ = 1/14 [30].

Let $\mathcal{C}(t, \chi)$ and $\mathcal{D}(t, \chi)$ represent the cumulative number of confirmed cases and cumulative number of deaths, respectively. The dynamic equations of $\mathcal{C}(t, \chi)$ and $\mathcal{D}(t, \chi)$ are as follows:

$$\begin{cases} \frac{d\mathcal{C}(t,\chi)}{dt} = \delta_I(t)I + \delta_q(t)E_q, \\ \frac{d\mathcal{D}(t,\chi)}{dt} = \mu(t)(I + H), \end{cases}$$

where χ represents an unknown parameter set. The daily confirmed cases and deaths are

$$\begin{cases} \mathcal{P}_{\mathcal{C}}(i, \chi) = \int_{\text{day } i} \left(\delta_I(t)I + \delta_q(t)E_q \right) dt, \\ \mathcal{P}_{\mathcal{D}}(i, \chi) = \int_{\text{day } i} \mu(t)(I + H) \, dt. \end{cases}$$
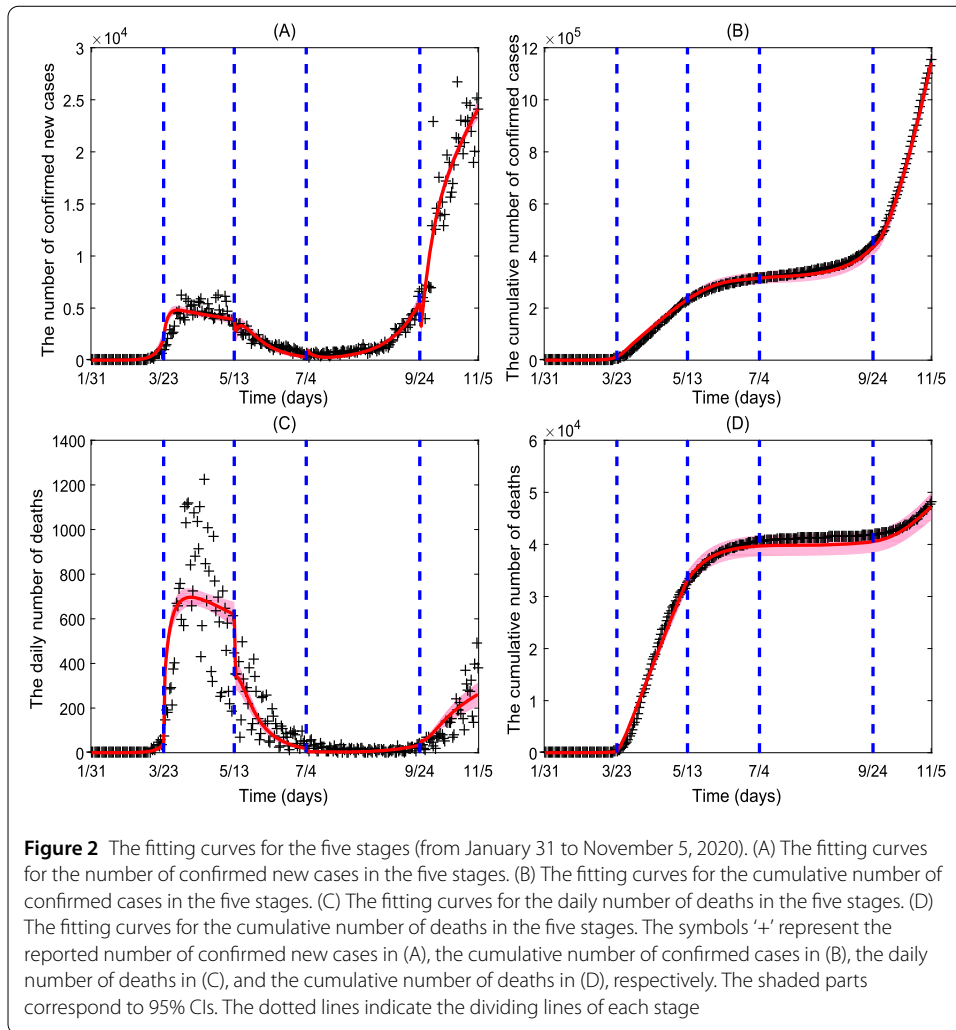
We used the MCMC method to estimate $\beta(t)$, $c(t)$, $\mu(t)$, $\delta_I(t)$, $q(t)$, and $\delta_q(t)$ by fitting the model to the number of confirmed new cases and daily number of deaths. Other parameters were kept constant, as listed in Table 1. We ran the DRAM algorithm for 20,000 iterations with the last 5000 iterations converged after the initial 'burn-in' period. The Geweke convergence diagnostic was employed to assess the convergence of chains. More details on the MCMC method can be found in Appendix A.

Figures 2(A)–(D) show the fitting curves for the number of confirmed new cases, the cumulative number of confirmed cases, the daily number of deaths, and the cumulative number of deaths in five stages from January 31 to November 5, 2020, respectively. The symbols '+' represent the reported number of confirmed new cases in (A), the cumulative number of confirmed cases in (B), the daily number of deaths in (C), and the cumulative number of deaths in (D), respectively. The shadow represents 95% confidence intervals (CIs). The dotted lines indicate the division of each stage. Figure 10 shows a high correlation between the number of estimated cases and the number of reported cases, indicating a good fitting effect.

MCMC approach provided the estimated mean value of $\beta(t)$, $c(t)$, $\mu(t)$, and $\delta_I(t)$ in five stages, $q(t)$ and $\delta_q(t)$ in three stages as shown in Table 1 and Figure 9. We used profile analysis to verify that all these parameters are identifiable when fitting this model to the data [32].

4 The effective reproduction number $R_e(t)$

The effective reproduction number, $R_e(t)$, is the mean number of secondary cases produced by an infected individual at any time, t, during an epidemic, which can be used to

Figure 2 The fitting curves for the five stages (from January 31 to November 5, 2020). (A) The fitting curves for the number of confirmed new cases in the five stages. (B) The fitting curves for the cumulative number of confirmed cases in the five stages. (C) The fitting curves for the daily number of deaths in the five stages. (D) The fitting curves for the cumulative number of deaths in the five stages. The symbols '+' represent the reported number of confirmed new cases in (A), the cumulative number of confirmed cases in (B), the daily number of deaths in (C), and the cumulative number of deaths in (D), respectively. The shaded parts correspond to 95% CIs. The dotted lines indicate the dividing lines of each stage

quantify the effectiveness of different mitigation strategies [33]. The effective reproduction numbers, $R_e(t)$ is

$$R_e(t) = R_e^E(t) + R_e^A(t) + R_e^I(t), \tag{2}$$

where

$$R_e^E(t) = \beta(t)c(t)\big(1 - q(t)\big)\frac{\nu}{\alpha}\frac{S(t)}{N(t)},$$

$$R_e^A(t) = \beta(t)c(t)\big(1 - q(t)\big)\frac{\theta(1 - \rho)}{\gamma_A}\frac{S(t)}{N(t)},$$

$$R_e^I(t) = \beta(t)c(t)\big(1 - q(t)\big)\frac{\rho}{\gamma_I + \delta_I(t) + \mu(t)}\frac{S(t)}{N(t)}.$$

Here, the effective reproduction numbers associated with the exposed population, $R_e^E(t)$, represents the number of secondary cases produced by an exposed infected individual at any time during the incubation period, where $\nu\beta(t)c(t)(1 - q(t))$ is the transmission rate
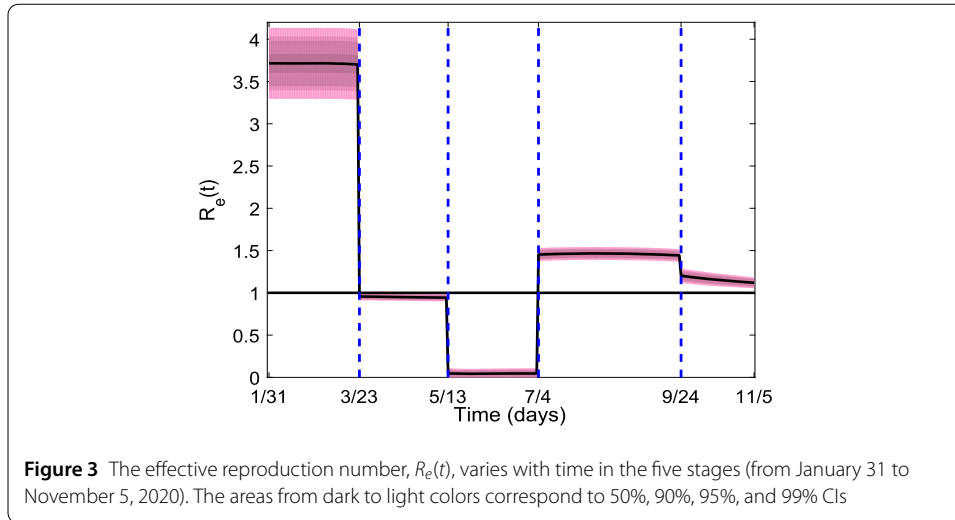
Figure 3 The effective reproduction number, $R_e(t)$, varies with time in the five stages (from January 31 to November 5, 2020). The areas from dark to light colors correspond to 50%, 90%, 95%, and 99% CIs

of exposed individuals who are missed through the contact tracing, and $1/\alpha$ is the average length of the incubation period.

The effective reproduction numbers associated with the asymptomatic infected population, $R_e^A(t)$, is the number of secondary cases produced by an asymptomatic infectious individual at any time during the asymptomatic infectious period. The factor $1 - \rho$ is the probability that an infectious individual is asymptomatic. In this expression, θ represents a reduction in the transmission rate of asymptomatic infectious individuals and $1/\gamma_A$ is the average length of the asymptomatic infectious period.
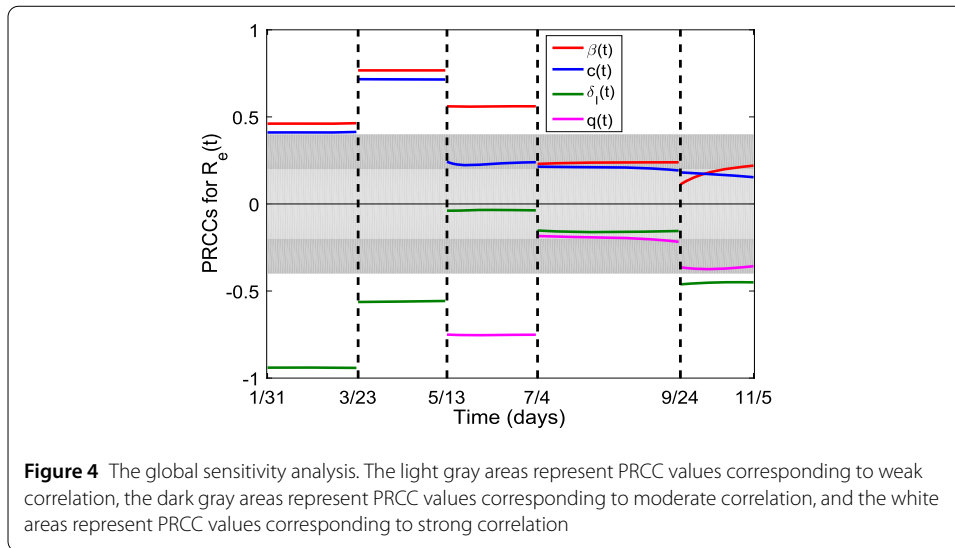
The effective reproduction numbers associated with the symptomatic infected population, $R_e^I(t)$, is the number of secondary cases produced by a symptomatic infectious individual during the infectious period, weighted by ρ, the probability that an infectious individual shows symptoms. Here, $1/(\gamma_I + \delta_I(t) + \mu(t))$ is the average length of the symptomatic infectious period. The values for each of these reproduction numbers can be approximated using the parameters estimated by the DRAM algorithm.

Figure 3 shows the effective reproduction number, $R_e(t)$, plotted as a function of time in each of the five stages. The areas from dark to light colors correspond to 50%, 90%, 95%, and 99% CIs. The mean values of for five stages are 3.7070 (95% CI: 3.3890−4.0255), 0.9500 (95% CI: 0.9216−0.9784), 0.0465 (95% CI: 0.0063−0.0867), 1.4470 (95% CI: 1.3990−1.5000), and 1.1605 (95% CI: 1.108−1.2075), respectively.

5 The global sensitivity analysis

We use the PRCC to study the global sensitivity of the parameters of Model (1). According to the estimated results of these parameters in Table 1, we choose a normal distribution for these parameters, where the mean and standard deviation are given in Table 1. The values of PRCCs for each stage are plotted in Figure 4 to show the importance of the parameters. The input parameters and output variables are positively (or negatively) correlated if the values of PRCCs are positive (or negative). The input parameters and output variables are strongly (moderately or weakly) correlated if the absolute values of PRCCs are between 0.4 and 1 (between 0.2 and 0.4 or between 0 and 0.2).

In Figure 4, the effective reproduction number, $R_e(t)$, and the transmission rate, $\beta(t)$, are strongly positively correlated in stages 1, 2, and 3, moderately positively correlated in

Figure 4 The global sensitivity analysis. The light gray areas represent PRCC values corresponding to weak correlation, the dark gray areas represent PRCC values corresponding to moderate correlation, and the white areas represent PRCC values corresponding to strong correlation
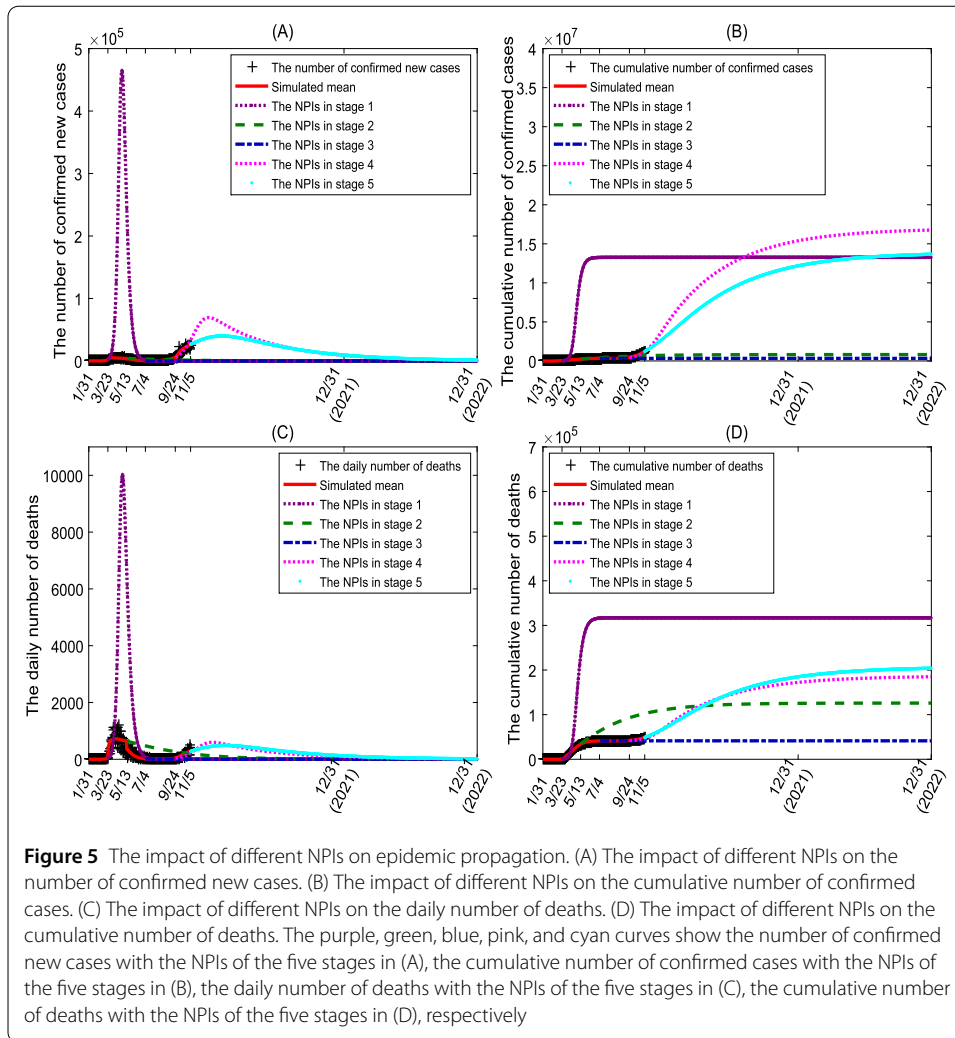
stage 4, and weakly correlated in stage 5. The effective reproduction number, $R_e(t)$, and the contact rate, $c(t)$, are strongly positively correlated in stages 1 and 2, moderately positively correlated in stages 3 and 4, and weakly correlated in stage 5. The effective reproduction number, $R_e(t)$, and the rate at which symptomatic infectious individuals are hospitalized, $\delta_I(t)$, are strongly negatively correlated in stages 1, 2, and 5, and weakly correlated in stages 3 and 4. The effective reproduction number, $R_e(t)$, and the quarantined proportion of close contacts, $q(t)$, are strongly negatively correlated in stage 3, moderately negatively correlated in stage 5, and weakly correlated in stage 4.

6 Predicting the epidemic propagation

Using our model with estimated parameters, we predict the trend of the early COVID-19 epidemic in the UK and evaluate the effectiveness of NPIs. In Figure 5(A), the purple curve shows that the number of confirmed new cases peaks on May 1, 2020, and the peak size is 465,000, if the NPIs of the first stage continue being implemented. The green curve shows that the number of confirmed new cases would be close to zero by November 18, 2022, if the NPIs of the second stage continue. The blue curve shows that the number of confirmed new cases would be close to zero by September 19, 2020, if the NPIs of the third stage continue. The pink curve shows that the number of confirmed new cases with the NPIs of the fourth stage peaks on December 25, 2020, and the peak size is 69,400. The cyan curve shows that the number of confirmed new cases peaks on January 31, 2021, and the peak size is 39,890 with the NPIs of the fifth stage.

In Figure 5(B), the purple curve shows that the final cumulative number of confirmed cases would be around 13,260,000, if the NPIs during the first stage continue. The green curve shows that the final cumulative number of confirmed cases would be around 817,100, if the NPIs in the second stage remain. The blue curve shows that the final cumulative number of confirmed cases would be around 330,700, if the NPIs in the third stage remain. The pink curve shows that the cumulative number of confirmed cases would be around 16,760,000 by the end of 2022, if the NPIs in the fourth stage remain. The cyan curve shows that the cumulative number of confirmed cases would be around 13,660,000 by the end of 2022, if the NPIs in the fifth stage remain.

Figure 5 The impact of different NPIs on epidemic propagation. (A) The impact of different NPIs on the number of confirmed new cases. (B) The impact of different NPIs on the cumulative number of confirmed cases. (C) The impact of different NPIs on the daily number of deaths. (D) The impact of different NPIs on the cumulative number of deaths. The purple, green, blue, pink, and cyan curves show the number of confirmed new cases with the NPIs of the five stages in (A), the cumulative number of confirmed cases with the NPIs of the five stages in (B), the daily number of deaths with the NPIs of the five stages in (C), the cumulative number of deaths with the NPIs of the five stages in (D), respectively

In Figure 5(C), the purple curve shows that the daily number of deaths peaks on May 2, 2020, and the peak size is 10,030 if the NPIs of the first stage continue. The green curve shows that the daily number of deaths would be close to zero by June 11, 2022, if the NPIs of the second stage continue. The blue curve shows that the daily number of deaths would be close to zero by September 7, 2020, if the NPIs of the third stage continue. The pink curve shows that the number of confirmed new cases peaks on January 5, 2021, and the peak size is 598 with the NPIs of the fourth stage. The cyan curve shows that the number of confirmed new cases peaks on February 10, 2021, and the peak size is 487 with the NPIs of the fifth stage.
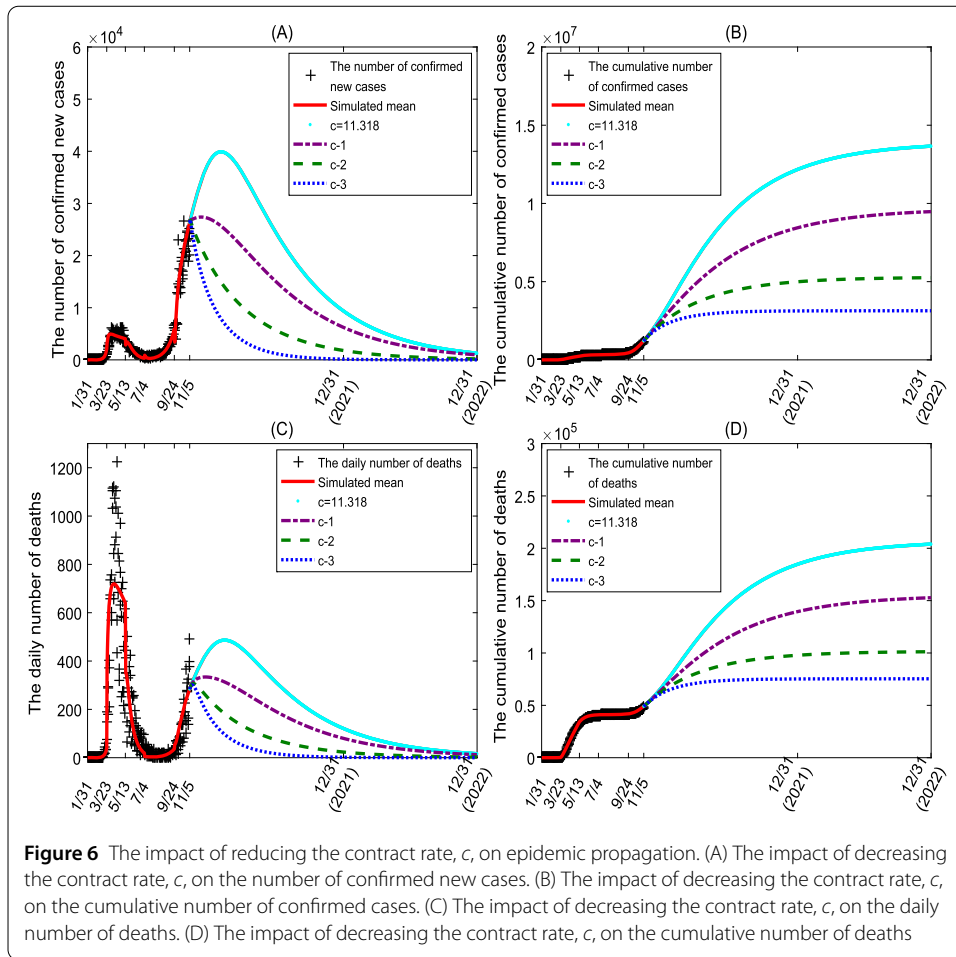
In Figure 5(D), the purple curve shows that the final cumulative number of deaths would be around 317,100, if the NPIs during the first stage continue. The green curve shows that the final cumulative number of deaths would be around 125,900, if the NPIs in the second stage remain. The blue curve shows that the final cumulative number of deaths would be around 41,360, if the NPIs in the third stage remain. The pink curve shows that the cumulative number of deaths would be around 185,000 by the end of 2022, if the NPIs in the fourth stage remain. The cyan curve shows that the cumulative number of deaths would be around 203,900 by the end of 2022, if the NPIs in the fifth stage remain.

The findings reveal the significant impact of NPIs on the dynamics of the disease spread. The higher peaks of confirmed new cases and daily deaths associated with the NPIs of the first stage emphasize the importance of implementing timely and stringent measures to mitigate the spread of the disease. The lower cumulative number of cases and deaths in the second and third stages underscores the effectiveness of NPIs in containing and managing the outbreak. Particularly, the lowest cumulative number of cases and deaths in the third stage signifies the critical role of NPIs at this phase. However, the proportion of deaths in the five stages is 2.4%, 15%, 13%, 1.1%, and 1.5%, respectively, which corresponds to the mortality rate $\mu(t)$ in the five stages, as shown in Figure 9. We found that although the cumulative number of cases and deaths in the second and third stages is lower than in other stages, the proportion of deaths is higher than in other stages. Moreover, the effectiveness of close contact tracing and lockdown measures in reducing the peaks of confirmed new cases and daily deaths highlights the proactive measures that can be taken to curb the impact of the disease. These findings emphasize the critical importance of implementing targeted and robust NPIs, alongside proactive contact tracing and stringent lockdown measures, in safeguarding public health and reducing the burden on healthcare systems.

From November 5, 2020, the community in the UK implemented lockdown again, which could reduce the transmission rate, $\beta(t)$, and the contact rate, $c(t)$. In Figures 11 and 6, we simulate the effect of lockdown.
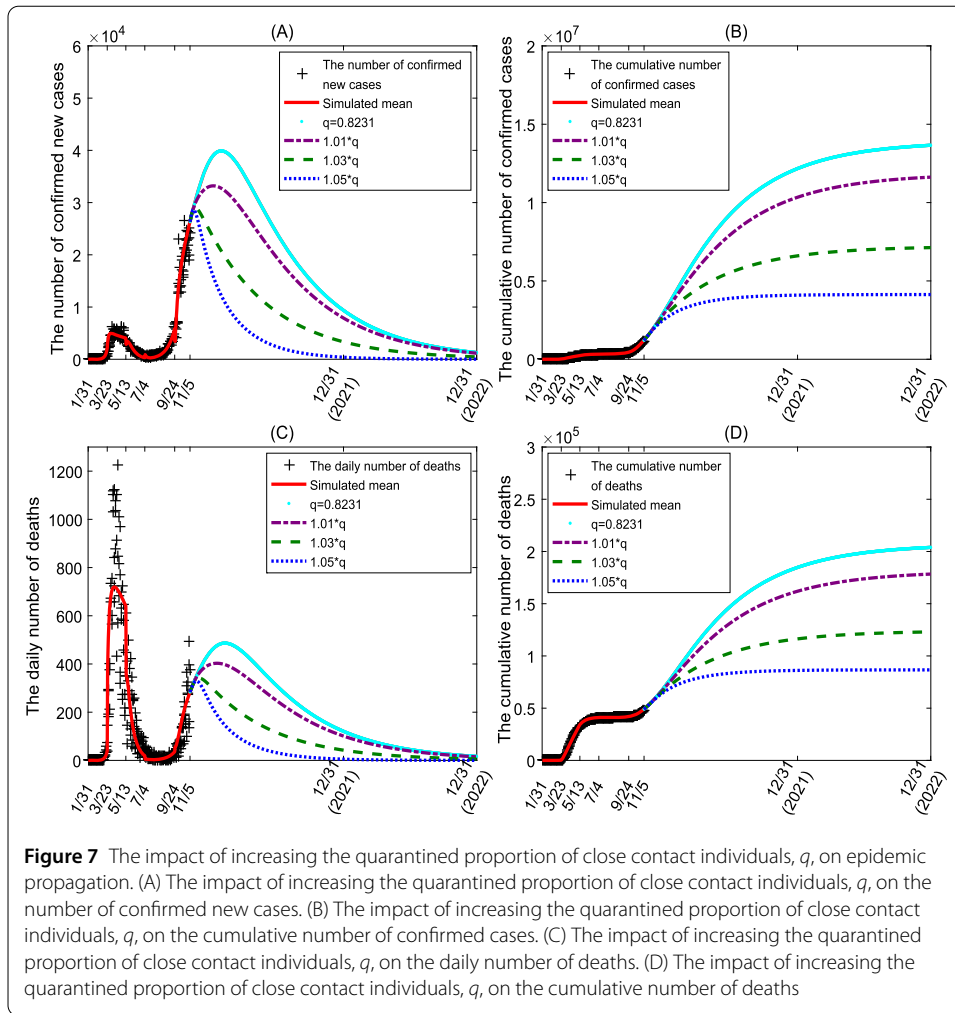
In Figure 11, the cyan curves display the daily number of confirmed cases in (A), the cumulative number of confirmed cases in (B), the daily number of deaths in (C), and the cumulative number of deaths in (D), assuming the NPIs in the fifth stage remain in effect with a given transmission rate ($\beta = 0.0658$). The purple, green, and blue dotted lines represent the projected statistics for the number of confirmed new cases in (A), the cumulative number of confirmed cases in (B), the daily number of deaths in (C), and the cumulative number of deaths in (D) when the transmission rates are reduced by 5%, 15%, and 45%, respectively. From a qualitative perspective, it is anticipated that by December 31, 2022, under the scenarios of reduced transmission rates, there will be noticeable decreases in the cumulative number of confirmed cases and deaths. Specifically, a 5% reduction in the transmission rate is expected to lead to a moderate decrease in both confirmed cases and deaths. A 15% reduction is projected to result in a significant reduction, while a 45% reduction is anticipated to have a substantial impact, with considerable decreases in both confirmed cases and deaths. These findings suggest that implementing measures to lower the transmission rate can have a positive influence on controlling the spread of the epidemic and mitigating its impact on public health.

In Figure 6, the cyan curves show the daily number of confirmed cases in (A), the cumulative number of confirmed cases in (B), the daily number of deaths in (C), and the cumulative number of deaths in (D) with NPIs at stage five remaining constant ($c = 11.318$). The purple, green, and blue dotted lines show the same variables when contact rates are reduced by one (e.g., $c = 11.318 - 1$), two (e.g., $c = 11.318 - 2$), and three (e.g., $c = 11.318 - 3$), respectively. By December 31, 2022, the cumulative number of confirmed cases will reduce by 30.63%, 61.54%, and 77.02%, respectively, and the cumulative number of deaths will reduce by around 25.06%, 50.37%, and 63.05%, respectively. We can anticipate that a reduction in contact rates will lead to a gradual decrease in the daily number of newly con-
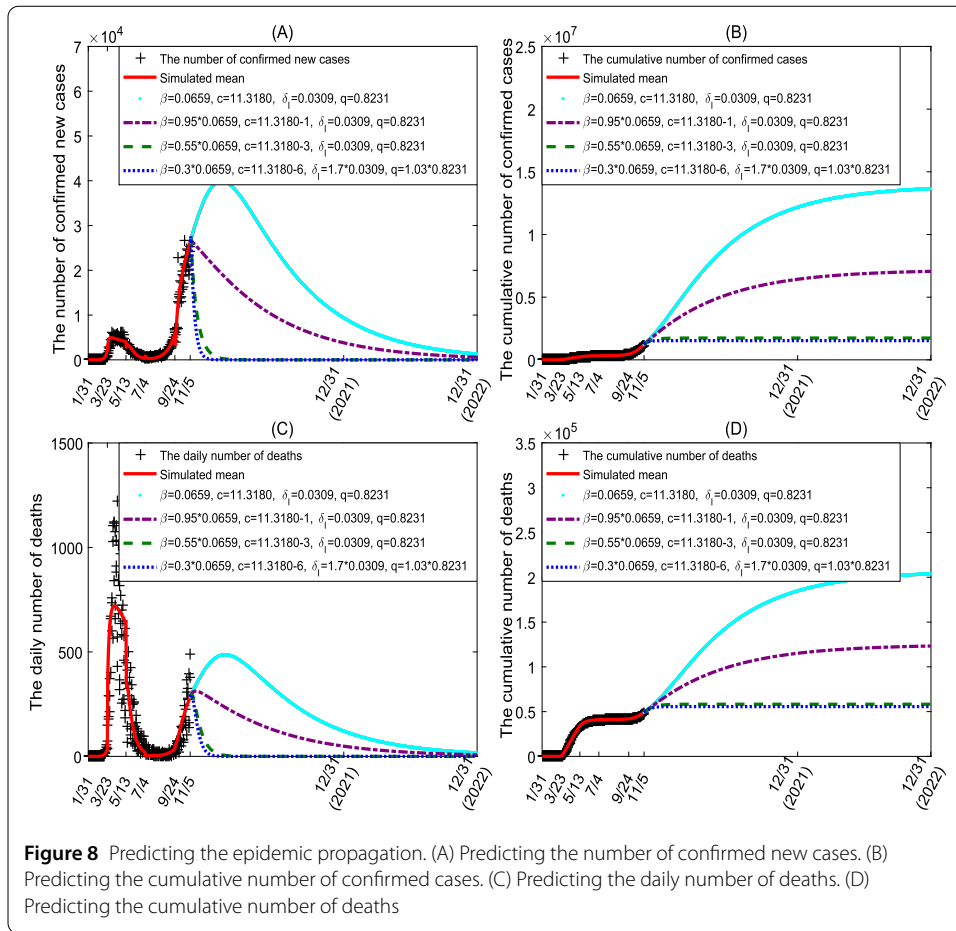
Figure 6 The impact of reducing the contract rate, *c*, on epidemic propagation. (A) The impact of decreasing the contract rate, *c*, on the number of confirmed new cases. (B) The impact of decreasing the contract rate, *c*, on the cumulative number of confirmed cases. (C) The impact of decreasing the contract rate, *c*, on the daily number of deaths. (D) The impact of decreasing the contract rate, *c*, on the cumulative number of deaths

firmed cases and daily deaths. This implies that altering the contact rates will slow down the spread of the disease and lower the overall number of cases. Moreover, the growth rates of cumulative confirmed cases and cumulative deaths will also be influenced, with larger reductions in contact rates resulting in more significant decreases. The qualitative analysis suggests that reducing contact rates will have a positive impact on disease transmission and case numbers, potentially slowing the spread of the outbreak and reducing mortality rates.

Next, we test the impact of the rate at which symptomatic infectious individuals are hospitalized and the quarantined proportion of close contacts on epidemic propagation. In Figure 12, we simulate the effect of increasing the rate of hospitalization for symptomatic infectious individuals, $\delta_I(t)$. The cyan curves show the daily number of confirmed cases in (A), the cumulative number of confirmed cases in (B), the daily number of deaths in (C), and the cumulative number of deaths in (D) with NPIs at stage five remaining constant ($\delta_I = 0.0309$). The purple, green, and blue dotted lines represent the same variables when $\delta_I(t)$ increases by 1.5, 2.5, and 5.5 times, respectively. We found that increasing the rate at which symptomatic infectious individuals are hospitalized can significantly affect the epidemic propagation. A higher hospitalization rate can lead to a decrease in the daily number of confirmed cases and deaths, as well as a reduction in the cumulative number of confirmed cases and deaths over time. Specifically, a higher hospitalization rate can result

Figure 7 The impact of increasing the quarantined proportion of close contact individuals, q, on epidemic propagation. (A) The impact of increasing the quarantined proportion of close contact individuals, q, on the number of confirmed new cases. (B) The impact of increasing the quarantined proportion of close contact individuals, q, on the cumulative number of confirmed cases. (C) The impact of increasing the quarantined proportion of close contact individuals, q, on the daily number of deaths. (D) The impact of increasing the quarantined proportion of close contact individuals, q, on the cumulative number of deaths

in a more rapid isolation and treatment of infected individuals, which in turn can reduce the spread of the disease within the community. This can lead to a decline in the overall number of cases and deaths, as well as a slower growth rate in the cumulative numbers. Furthermore, by quarantining a higher proportion of close contacts, there can be a further reduction in the transmission of the disease. This can potentially limit the number of new cases and decrease the overall impact of the epidemic.

In Figure 7, we simulate the effect of increasing the quarantined proportion of close contacts, $q(t)$. The cyan curves show the daily number of confirmed cases in (A), the cumulative number of confirmed cases in (B), the daily number of deaths in (C), and the cumulative number of deaths in (D), if the NPIs in the fifth stage remain ($q = 0.8231$). The purple, green, and blue dotted lines represent the number of confirmed new cases in (A), the cumulative number of confirmed cases in (B), the daily number of deaths in (C), and the cumulative number of deaths in (D), when the quarantined proportion of close contact individual, $q(t)$, increases by 1%, 3%, and 5%, respectively. We found that increasing the proportion of quarantine for close contacts may have a significant impact on the spread of the epidemic. By isolating close contacts more widely, it may effectively reduce the spread of the virus within the community, thereby lowering the daily number of confirmed cases and deaths. A higher quarantine proportion may lead to the cutting off

Figure 8 Predicting the epidemic propagation. (A) Predicting the number of confirmed new cases. (B) Predicting the cumulative number of confirmed cases. (C) Predicting the daily number of deaths. (D) Predicting the cumulative number of deaths

of more potential chains of virus transmission, thus slowing the spread of the epidemic. This could potentially decrease the number of new cases and reduce the risk of infection within the community. Additionally, increasing the quarantine for close contacts may limit the continued spread of the epidemic, thereby reducing the strain on medical resources and systems. This could help in reducing the cumulative number of confirmed cases and deaths.

Finally, we predict the epidemic propagation under different scenarios. In Figure 8, the cyan curves show the daily number of confirmed cases in (A), the cumulative number of confirmed cases in (B), the daily number of deaths in (C), and the cumulative number of deaths in (D), if the NPIs in the fifth stage remain ($\beta = 0.0659$, $c = 11.318$, $\delta_I = 0.0309$, and $q = 0.8231$). The purple dotted lines represent the number of confirmed new cases in (A), the cumulative number of confirmed cases in (B), the daily number of deaths in (C), and the cumulative number of deaths in (D), when $\beta = 0.95 \times 0.0659$, $c = 11.318 - 1$, $\delta_I = 0.0309$, and $q = 0.8231$. The green dotted lines represent the number of confirmed new cases in (A), the cumulative number of confirmed cases in (B), the daily number of deaths in (C), and the cumulative number of deaths in (D), when $\beta = 0.55 \times 0.0659$, $c = 11.318 - 3$, $\delta_I = 0.0309$, and $q = 0.8231$. The blue dotted lines represent the number of confirmed new cases in (A), the cumulative number of confirmed cases in (B), the daily number of deaths in (C), and the cumulative number of deaths in (D), when $\beta = 0.3 \times 0.0659$, $c = 11.318 - 6$,

$\delta_I = 1.7 \times 0.0309$, and $q = 1.03 \times 0.8231$, where the values of β, c, and δ_I are approximate to the second stage ($\beta = 0.0197$, $c = 5.6702$, and $\delta_I = 0.0536$, as shown in Table 1).

The predictions suggest that implementing different levels of interventions can have a significant impact on reducing the spread of the disease and lowering the associated mortality by December 31, 2022. Under the purple scenario, which represents a moderate decrease in transmission and contact rates, there is an expected decrease in the cumulative number of confirmed cases by approximately 48.32%. This indicates that even small reductions in transmission and contact rates can lead to a noticeable decrease in the spread of the disease. The green and blue scenarios, with more substantial decreases in transmission and contact rates as well as an increase in isolation rate, show even larger reductions in the cumulative number of confirmed cases, by approximately 87.25% and 88.78% respectively. This suggests that implementing more aggressive interventions can result in a drastic reduction in the spread of the disease within the population. Furthermore, under all scenarios, there is an expected decrease in the cumulative number of deaths by approximately 39.53%, 71.44%, and 72.73% under the purple, green, and blue scenarios, respectively. This indicates that these interventions can also have a positive impact on reducing mortality associated with the disease, and the more intensive interventions have a greater potential for saving lives.

In summary, the findings indicate that even small reductions in transmission and contact rates can lead to a noticeable decrease in the spread of the disease, while more aggressive interventions can result in a significant reduction in both the spread of the disease and its associated mortality. These results highlight the potential impact of different levels of interventions in managing the disease outbreak.

7 Discussion and conclusions

We fitted our compartmental differential equation model to the number of confirmed new cases and daily number of deaths in the five stages from January 31 to November 5, 2020.

The model projections indicated that if the NPIs in the fifth stage remained, the epidemic could last more than two years. In this case, the cumulative number of confirmed cases would be around 13,660,000, and the cumulative number of deaths would be around 203,900 by December 31, 2022.

The simulations also showed that if community lockdown started from November 5, 2020, the transmission rate, the contact rate, and the rate at which symptomatic infectious individuals are hospitalized were approximately equal to those in the second stage of the most strict NPIs, and the proportion of quarantined close contacts increased by 3%, then the epidemic could die out as early as January 12, 2021, the final cumulative number of confirmed cases would be around 1,533,000, as shown in Figure 8(B), and the final cumulative number of deaths would be around 55,610, as shown in Figure 8(D). On November 5, 2020, the UK did not implement NPIs as strictly as the second stage. Hence, we assumed the transmission rate reduced by 45%, the contact rate reduced by 26.5%, the hospitalization rate and proportion of quarantined close contacts were the same as those in the fifth stage, then the epidemic could die out around July 4, 2021, the final cumulative number of confirmed cases would be around 1,741,000, and the final cumulative number of deaths would be around 58,240. Finally, we assumed that the UK implemented weak interventions from November 5, 2020, that were, the transmission rate decreased by 5%, the contact rate reduced by 8.84%, the hospitalization rate and proportion of quarantined

close contacts were the same as those in the fifth stage, then the epidemic could last more than two years, the cumulative number of confirmed cases would be around 7,060,000, and the cumulative number of deaths would be around 123,300 by December 31, 2022. Even if the weak NPIs were implemented, the cumulative number of confirmed cases would reduce by 48.32%, and the cumulative number of deaths would reduce by around 39.53% by December 31, 2022. Hence, the NPIs could save a large number of lives.

Here, we demonstrated data-driven studies, assuming that multiple NPIs including but not limited to quarantine, contact tracing, social distancing, self-isolation, and community lockdown. The health and economic impacts of different interventions need to be balanced in the short and long term in any society. The epidemiological data implied that no country had yet seen enough infections to prevent the second wave of transmission by herd immunity if lockdown interventions were relaxed by November 2020.

The dynamics of person-to-person transmission are mainly driven by contacts between individuals [34, 35], which can be heterogeneous due to age and location, and to viral loads of infected individuals. Once the travel restrictions are lifted, human mobility will contribute to the rapid epidemic propagation within the UK [36].

In our study, we found that NPIs such as quarantine, contact tracing, social distancing, self-isolation, and community lockdown play a crucial role in controlling the spread of epidemics. This is consistent with the findings of previous studies [37–39]. The data-driven studies presented in our study highlight the potential of these interventions to significantly impact the trajectory of the epidemic. It is clear that while these NPIs can have profound health benefits in terms of reducing the cumulative number of confirmed cases and deaths, the economic and social impacts also need to be considered. Our simulation results emphasize the need to balance the short-term and long-term effects of these interventions on both health and the economy. Additionally, the study underscores the importance of continued vigilance and caution, as lifting lockdown interventions too early could potentially lead to a second wave of transmission. Overall, the dynamic nature of person-to-person transmission and the influence of human mobility after travel restrictions are lifted further emphasize the significance of effective NPIs in mitigating epidemic propagation.

These projections all depend on the sensitivity of the simulations to the model assumptions. Our model did not account for the heterogeneity in the behavior of individuals, the population density, or the disease mortality as a function of age. We are continuing to refine our model to understand the impact of these effects and capture them more realistically in future models.

Appendix A: MCMC method for parameter estimation

Let ε represent the fitting error, following an independent Gaussian distribution with a mean of zero and unknown variance ξ^2, as per the Central Limit Theorem. Accordingly, the observations y can be expressed as

$$y = f(x, \chi) + \varepsilon, \quad \varepsilon \sim N\left(0, I\xi^2\right). \tag{3}$$

Here, $f(x, \chi)$ denotes the nonlinear model ($\mathcal{P}_\mathcal{C}(i, \chi)$ and $\mathcal{P}_\mathcal{D}(i, \chi)$), x represents the independent variables, and χ stands for the unknown parameters and initial values. For sim-

plicity, we assume that the unknown parameters χ of the system are independent Gaussian prior specifications. Therefore, we have

$$\hat{\chi}_j \sim N\left(\nu_j, \varphi_j^2\right), \quad j = 1, \ldots, M,$$

where M is the number of unknown parameters. Additionally, we further assume that the inverse of the error variance follows a gamma distribution as a prior with the form

$$p\left(\xi^{-2}\right) \sim \Gamma\left(\frac{n_0}{2}, \frac{n_0}{2} S_0^2\right),$$

where S_0^2 and n_0 are the prior mean and accuracy of the variance ξ^2, respectively.

The likelihood function $p(y|\chi, \xi^2)$ for Ψ independent identically distributed observations with a Gaussian error model is

$$p\left(y|\chi, \xi^2\right) = \left(\frac{1}{\sqrt{2\pi\xi^2}}\right)^{\Psi} \exp\left[\frac{-SS(\chi)}{2\xi^2}\right],$$

where $SS(\chi)$ represents the sum of squares function

$$SS(\chi) = \sum_{i=1}^{\Psi}\left[y_i - f(\chi)_i)^2\right].$$

The conditional distribution $p(\xi^{-2}|y, \chi)$ can be expressed as follows:

$$p\left(\xi^{-2}|y, \chi\right) \propto p\left(y|\xi^{-2}, \chi\right) p\left(\xi^{-2}\right)$$

$$= \left(\frac{1}{\sqrt{2\pi\xi^{-1}}}\right)^{\Psi} \exp\left[\frac{-SS(\chi)}{2\xi^{-2}}\right] \frac{\left(\frac{n_0}{2} S_0^2\right)^{\frac{n_0}{2}}}{\Gamma\left(\frac{n_0}{2}\right)} \left(\xi^{-2}\right)^{-\frac{n_0}{2}-1} \exp\left[-\frac{n_0 S_0^2}{2\xi^{-2}}\right]$$

$$\propto \left(\xi^{-2}\right)^{-\frac{\Psi+n_0}{2}-1} \exp\left[-\frac{SS(\chi) + n_0 S_0^2}{2\xi^{-2}}\right].$$

According to the conditional conjugacy property of the Gamma distribution [40], the conditional distribution $p(\xi^{-2}|y, \chi)$ is also a Gamma distribution with the following parameters:

$$p\left(\xi^{-2}|y, \chi\right) = \Gamma\left(\frac{\Psi + n_0}{2}, \frac{SS(\chi) + n_0 S_0^2}{2}\right).$$

This is used to sample and update ξ^{-2} for other parameters within each run of Metropolis–Hastings (MH) simulation steps. Assuming independent Gaussian prior specification for parameters χ, the prior sum of squares for the given parameters χ can be calculated as follows:

$$SS_{pri}(\chi) = \sum_{i=1}^{M}\left[\frac{\chi_i - \nu_i}{\varphi_i}\right]^2.$$

Hence, for a fixed value of variance ξ^2, the posterior distribution of parameters χ can be expressed as follows:

$$p(\chi|y,\xi^2)$$

$$\propto p(y|\chi,\xi^2)p(\chi_1)p(\chi_2)\cdots p(\chi_M) = p(\bar{Y}_C|\chi,\xi^2)\prod_{i=1}^{M}p(\chi_i)$$

$$= \left(\frac{1}{\sqrt{2\pi\xi^2}}\right)^{\Psi}\exp\left[\frac{-\mathrm{SS}(\chi)}{2\xi^2}\right]\prod_{j=1}^{M}\frac{1}{\sqrt{2\pi}\,\varphi_j}\exp\left[-\frac{(\chi_j-\nu_j)^2}{2\varphi_j^2}\right]$$

$$= \left(\frac{1}{\sqrt{2\pi\xi^2}}\right)^{\Psi}\exp\left[\frac{-\mathrm{SS}(\chi)}{2\xi^2}\right]\left(\frac{1}{\sqrt{2\pi}}\right)^{M}\frac{1}{\varphi_1\varphi_2\cdots\varphi_M}\exp\left[-\frac{1}{2}\sum_{j=1}^{M}\left(\frac{\chi_j-\nu_j}{\varphi_j}\right)^2\right]$$

$$\propto \exp\left[-\frac{1}{2}\left(\frac{\mathrm{SS}(\chi)}{\xi^2}+\mathrm{SS}_{\mathrm{pri}}(\chi)\right)\right],$$

and the posterior ratio needed in the MH acceptance probability can be written as follows:

$$\frac{p(\chi'|y,\xi^2)}{p(\chi|y,\xi^2)} = \exp\left[-\frac{1}{2}\left(\frac{\mathrm{SS}(\chi)}{\xi^2}-\frac{\mathrm{SS}(\chi')}{\xi^2}\right)+\frac{1}{2}\left(\mathrm{SS}_{\mathrm{pri}}(\chi)-\mathrm{SS}_{\mathrm{pri}}(\chi')\right)\right].$$

Accordingly, the new unknown parameter value χ will be accepted with probability

$$\min\left(1,\frac{p(\chi'|y,\xi^2)}{p(\chi|y,\xi^2)}\right).$$

In addition, if asymmetric distribution is chosen as the proposal distribution, the acceptance probability is

$$\min\left(1,\frac{p(\chi'|y,\xi^2)\mathbf{q}(\chi,\chi')}{p(\chi|y,\xi^2)\mathbf{q}(\chi',\chi)}\right).$$

Next, we give the details of Delaying Rejection [22]. Suppose the current position of the Markov chain is $X_t = x$. As in a regular MH, a candidate move G_1 is generated from a proposal $q_1(x,\cdot)$ and accepted with the usual probability

$$\alpha_1(x,g_1) = \min\left(1,\frac{p(g_1)q_1(g_1,x)}{p(x)q_1(x,g_1)}\right) = \min\left(1,\frac{\mathfrak{N}_1}{\mathfrak{D}_1}\right). \tag{4}$$

After a rejection, rather than remaining at the same position, $X_{t+1} = x$, as in a standard MH algorithm, a second stage move G_2 is suggested. This second stage proposal can be based not only on the current position of the chain but also on the previously proposed and rejected value: $q_2(x,g_1,\cdot)$. The acceptance of the second stage proposal occurs with a probability denoted by

$$\alpha_2(x,g_1,g_2) = \min\left(1,\frac{p(g_2)q_1(g_2,g_1)q_2(g_2,g_1,x)[1-\alpha_1(g_2,g_1)]}{p(x)q_1(x,g_1)q_2(x,g_1,g_2)[1-\alpha_1(x,g_1)]}\right)$$

$$= \min\left(1,\frac{\mathfrak{N}_2}{\mathfrak{D}_2}\right). \tag{5}$$

This process of delaying rejection can be iterated and the ith stage acceptance probability is

$$
\begin{aligned}
\alpha_i(x, g_1, \ldots, g_i) &= \min\Bigg(1, \frac{p(g_i)q_1(g_i, g_{i-1})q_2(g_i, g_{i-1}, g_{i-2}) \cdots q_i(g_i, g_{i-1}, \ldots, x)}{p(x)q_1(x, g_1)q_2(x, g_1, g_2) \cdots q_i(x, g_1, \ldots, g_i)} \\
&\quad \times \frac{[1 - \alpha_1(g_i, g_{i-1})][1 - \alpha_2(g_i, g_{i-1}, g_{i-2})] \cdots [1 - \alpha_{i-1}(g_i, \ldots, g_1)]}{[1 - \alpha_1(x, g_1)][1 - \alpha_2(x, g_1, g_2)] \cdots [1 - \alpha_{i-1}(x, g_1, \ldots, g_{i-1})]} \Bigg) \\
&= \min\left(1, \frac{\mathfrak{N}_i}{\mathfrak{D}_i} \right).
\end{aligned}
\tag{6}
$$

If the ith stage is reached, it means that $\mathfrak{N}_j < \mathfrak{D}_j$ for $j = 1, \ldots, i - 1$. Therefore, $\alpha_j(x, g_i, \ldots, g_j)$ can be rewritten as $\mathfrak{N}_j/\mathfrak{D}_j, j = 1, \ldots, i-1$, and we obtain the recursive formula

$$
\mathfrak{D}_i = q_i(x, \ldots, g_i)(\mathfrak{D}_{i-1} - \mathfrak{N}_{i-1})
$$

which leads to

$$
\begin{aligned}
\mathfrak{D}_i &= q_i(x, \ldots, g_i)\big[q_{i-1}(x, \ldots, g_{i-1})\big[q_{i-2}(x, \ldots, g_{i-2}) \\
&\quad \cdots \big[q_2(x, g_1, g_2)\big[q_1(x, g_1)\pi(x) - \mathfrak{N}_1\big] - \mathfrak{N}_2\big] - \mathfrak{N}_3\big] \cdots - \mathfrak{N}_{i-1}\big].
\end{aligned}
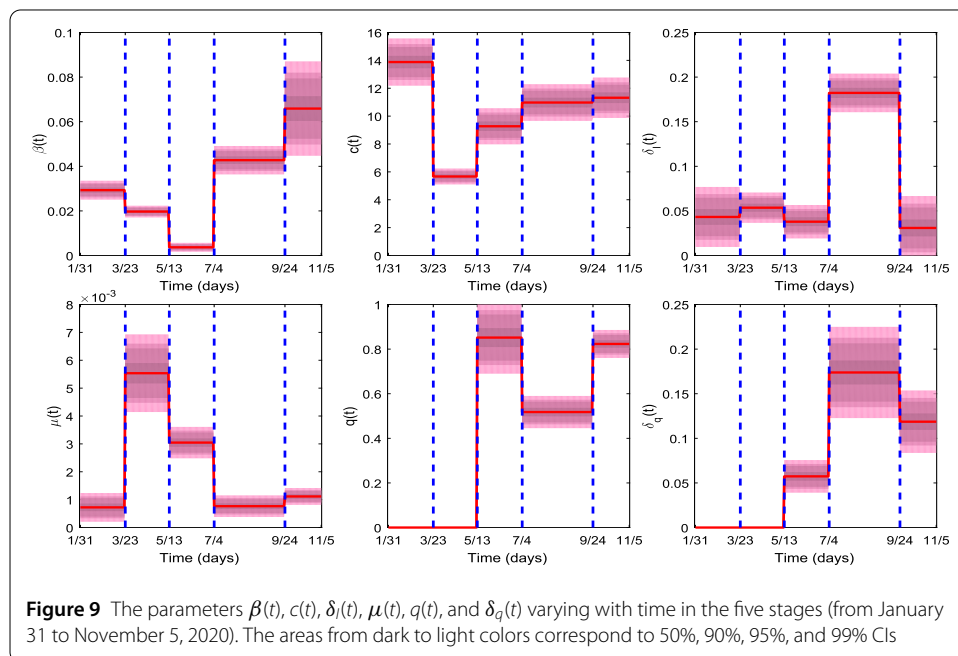\tag{7}
$$

Appendix B: Additional figures

Figure 9 The parameters $\beta(t)$, $c(t)$, $\delta_l(t)$, $\mu(t)$, $q(t)$, and $\delta_q(t)$ varying with time in the five stages (from January 31 to November 5, 2020). The areas from dark to light colors correspond to 50%, 90%, 95%, and 99% CIs
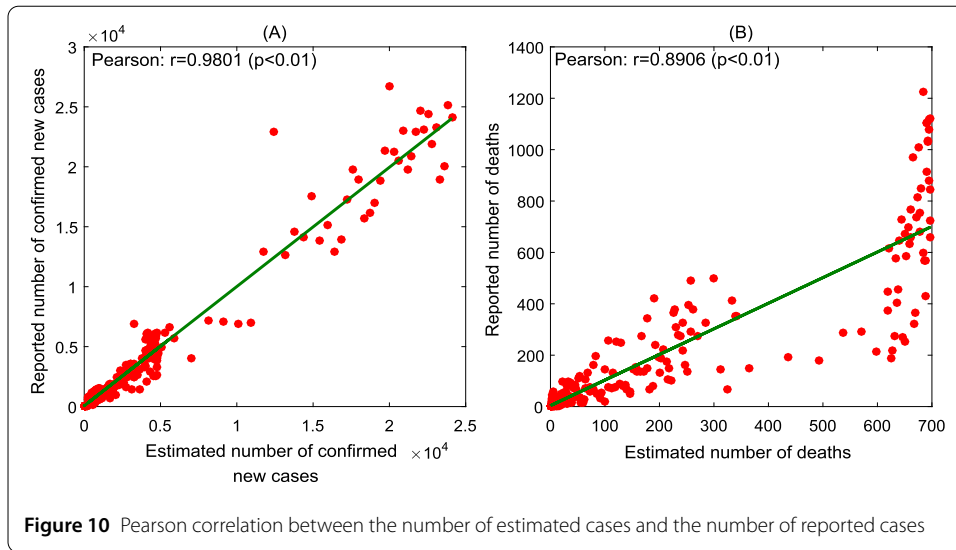
Figure 10 Pearson correlation between the number of estimated cases and the number of reported cases
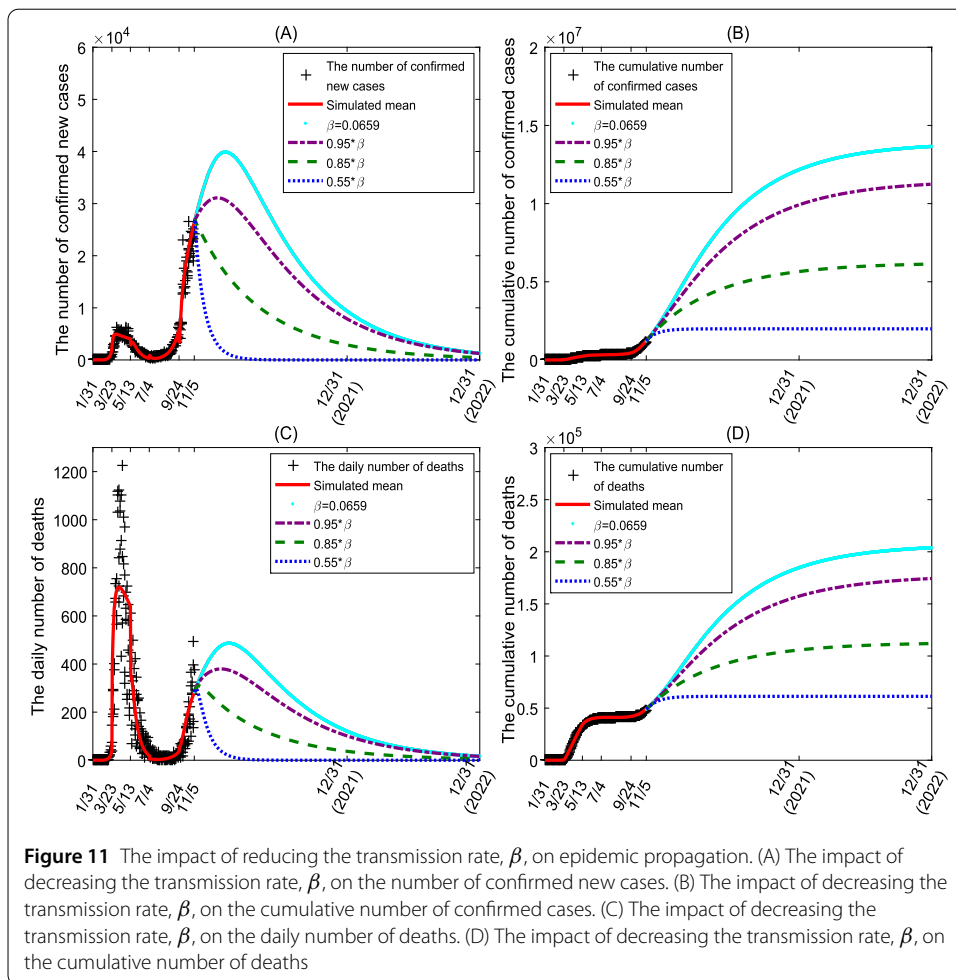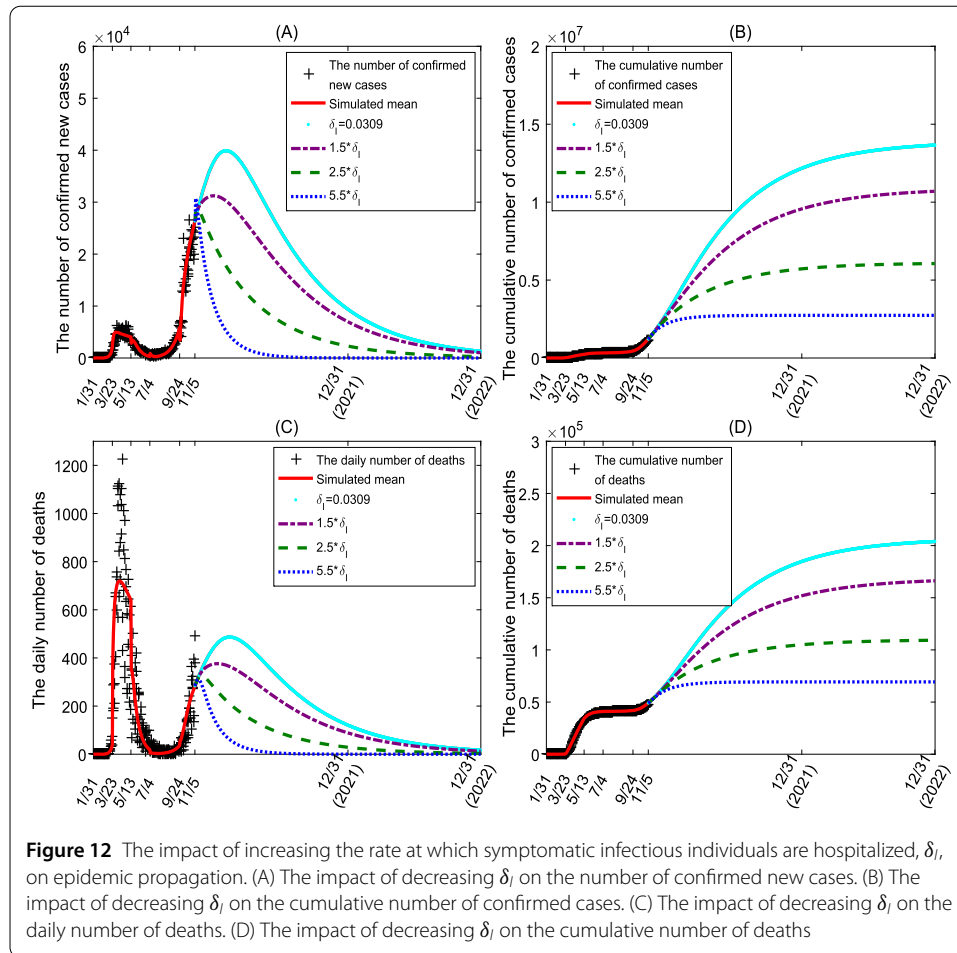

Figure 11 The impact of reducing the transmission rate, β, on epidemic propagation. (A) The impact of decreasing the transmission rate, β, on the number of confirmed new cases. (B) The impact of decreasing the transmission rate, β, on the cumulative number of confirmed cases. (C) The impact of decreasing the transmission rate, β, on the daily number of deaths. (D) The impact of decreasing the transmission rate, β, on the cumulative number of deaths

Figure 12 The impact of increasing the rate at which symptomatic infectious individuals are hospitalized, δ_I, on epidemic propagation. (A) The impact of decreasing δ_I on the number of confirmed new cases. (B) The impact of decreasing δ_I on the cumulative number of confirmed cases. (C) The impact of decreasing δ_I on the daily number of deaths. (D) The impact of decreasing δ_I on the cumulative number of deaths

Availability of data and materials
The data described in the current study can be freely and openly accessed via https://coronavirus.data.gov.uk/

Declarations

Competing interests
The authors declare that they have no competing interests.

Author contributions
The main idea of this paper was proposed by HZ and SJ. HZ prepared the manuscript initially. SJ implemented the simulations using the software. All authors read and approved the final manuscript.

Author details
[1]College of Mathematical Sciences, Mudanjiang Normal University, Mudanjiang, Heilongjiang, 157011, China. [2]College of Mathematical Sciences, Harbin Engineering University, Harbin, Heilongjiang, 150001, China.

References

1. Prem, K., Liu, Y., Russell, T.W., et al.: The effect of control strategies to reduce social mixing on outcomes of the COVID-19 epidemic in Wuhan, China: a modelling study. Lancet Public Health **5**(5), e261–e270 (2020)
2. UK Government: Coronavirus (COVID-19) in the UK. Available from: https://coronavirus.data.gov.uk/. Accessed 5 November 2020
3. Yang, X., Yu, Y., Xu, J., et al.: Clinical course and outcomes of critically ill patients with SARS-CoV-2 pneumonia in Wuhan, China: a single-centered, retrospective, observational study. Lancet Respir. Med. **8**(5), 475–481 (2020)
4. Guan, W., Ni, Z., Hu, Y., et al.: Clinical characteristics of coronavirus disease 2019 in China. N. Engl. J. Med. **382**(18), 1708–1720 (2020)
5. Gandhi, M., Yokoe, D.S., Havlir, D.V.: Asymptomatic transmission, the Achilles' heel of current strategies to control COVID-19. N. Engl. J. Med. **382**(22), 2158–2160 (2020)
6. Lavezzo, E., Franchin, E., Ciavarella, C., et al.: Suppression of a SARS-CoV-2 outbreak in the Italian municipality of Vo'. Nature **584**(7821), 425–429 (2020)
7. Johns Hopkins University Bloomberg School of Public Health: Global Health Security Index finds gaps in preparedness for epidemics and pandemics: even high-income countries are found lacking and score only in the average range of preparedness. Available from: https://www.sciencedaily.com/releases/2019/10/191024115022.htm. Accessed 17 July 2020
8. Jia, Z., Lu, Z.: Modelling COVID-19 transmission: from data to intervention. Lancet Infect. Dis. **20**(7), 757–758 (2020)
9. Grosios, K., Gahan, P.B., Burbidge, J.: Overview of healthcare in the UK. EPMA J. **1**(4), 529–534 (2010)
10. Banatvala, J.: COVID-19 testing delays and pathology services in the UK. Lancet **395**(10240), 1831 (2020)
11. Horton, R.: Offline: COVID-19 and the NHS-"a national scandal". Lancet **395**(10229), 1022 (2020)
12. Nishiura, H., Chowell, G.: The Effective Reproduction Number as a Prelude to Statistical Estimation of Time-Dependent Epidemic Trends, pp. 103–121. Springer, Netherlands (2009)
13. Treibel, T.A., Manisty, C., Burton, M., et al.: COVID-19: PCR screening of asymptomatic health-care workers at London hospital. Lancet **395**(10237), 1608–1610 (2020)
14. Wearing, H.J., Rohani, P., Keeling, M.J.: Appropriate models for the management of infectious diseases. PLoS Med. **2**(7), e174 (2005)
15. Siettos, C.I., Russo, L.: Mathematical modeling of infectious disease dynamics. Virulence **4**(4), 295–306 (2013)
16. He, D., Lin, L., Artzy-Randrup, Y., et al.: Resolving the enigma of Iquitos and Manaus: a modeling analysis of multiple COVID-19 epidemic waves in two Amazonian cities. Proc. Natl. Acad. Sci. **120**(10), e2211422120 (2023)
17. Keeling, M.J., Eames, K.T.: Networks and epidemic models. J. R. Soc. Interface **2**(4), 295–307 (2005)
18. Reppas, A.I., Spiliotis, K.G., Siettos, C.I.: Epidemionics: from the host-host interactions to the systematic analysis of the emergent macroscopic dynamics of epidemic networks. Virulence **1**(4), 338–349 (2010)
19. Xue, L., Jing, S., Miller, J.C., et al.: A data-driven network model for the emerging COVID-19 epidemics in Wuhan, Toronto and Italy. Math. Biosci. **326**, 108391 (2020)
20. Tang, B., Wang, X., Li, Q., et al.: Estimation of the Transmission Risk of the 2019-nCoV and Its Implication for Public Health Interventions. J. Clin. Med. **9**(2), 462–474 (2020)
21. Arnold, A.: Sequential Monte Carlo parameter estimation for differential equations, Case Western Reserve University (2014)
22. Haario, H., Laine, M., Mira, A., et al.: DRAM: Efficient adaptive MCMC. Stat. Comput. **16**(4), 339–354 (2006)
23. Wiersinga, W.J., Rhodes, A., Cheng, A.C., et al.: Pathophysiology, transmission, diagnosis, and treatment of coronavirus disease 2019 (COVID-19): a review. JAMA **324**(8), 782–793 (2020)
24. Lewer, D., Braithwaite, I., Bullock, M., et al.: COVID-19 among people experiencing homelessness in England: a modelling study. Lancet Respir. Med. **8**(12), 1181–1191 (2020)
25. Young, B.E., Ong, S.W.X., Kalimuddin, S., et al.: Epidemiologic features and clinical course of patients infected with SARS-CoV-2 in Singapore. JAMA **323**(15), 1488–1494 (2020)
26. Karagiannidis, C., Mostert, C., Hentschker, C., et al.: Case characteristics, resource use, and outcomes of 10021 patients with COVID-19 admitted to 920 German hospitals: an observational study. Lancet Respir. Med. **8**(9), 853–862 (2020)
27. Hu, Z., Song, C., Xu, C., et al.: Clinical characteristics of 24 asymptomatic infections with COVID-19 screened among close contacts in Nanjing, China. Sci. China Life Sci. **63**(5), 706–711 (2020)
28. Kucharski, A.J., Klepac, P., Conlan, A.J.K., et al.: Effectiveness of isolation, testing, contact tracing, and physical distancing on reducing transmission of SARS-CoV-2 in different settings: a mathematical modelling study. Lancet Infect. Dis. **20**(10), 1151–1160 (2020)
29. Zhang, Y., You, C., Cai, Z., et al.: Prediction of the COVID-19 outbreak in China based on a new stochastic dynamic model. Sci. Rep. **10**(1), 21522 (2020)
30. UK Government: Government launches NHS Test and Trace service. Available from: https://www.gov.uk/government/news/government-launches-nhs-test-and-trace-service. Accessed 27 May 2020
31. World Health Organization: United Kingdom. Available from: https://www.who.int/countries/gbr/en/. Accessed 13 May 2020
32. Raue, A., Maiwald, T., Timmer, J., et al.: Addressing parameter identifiability by model-based experimentation. IET Syst. Biol. **5**(2), 120–130 (2011)
33. Xue, L., Fang, X., Hyman, J.M.: Comparing the effectiveness of different strains of Wolbachia for controlling Chikungunya, Dengue fever, and Zika. PLoS Negl. Trop. Dis. **12**(7), e0006666 (2018)
34. Riou, J., Althaus, C.L.: Pattern of early human-to-human transmission of Wuhan 2019 novel coronavirus (2019-nCoV), December 2019 to January 2020. Euro Surveill. **25**(4), 2000058 (2020)
35. Chan, J.F.W., Yuan, S., Kok, K.H., et al.: A familial cluster of pneumonia associated with the 2019 novel coronavirus indicating person-to-person transmission: a study of a family cluster. Lancet **395**(10223), 514–523 (2020)
36. Wells, C.R., Sah, P., Moghadas, S.M., et al.: Impact of international travel and border control measures on the global spread of the novel 2019 coronavirus outbreak. Proc. Natl. Acad. Sci. **117**(13), 7504–7509 (2020)
37. Spiliotis, K., Koutsoumaris, C.C., Reppas, A.I., et al.: Optimal vaccine roll-out strategies including social distancing for pandemics. iScience **25**(7), 104575 (2022)
38. Armaou, A., Katch, B., Russo, L., et al.: Designing social distancing policies for the COVID-19 pandemic: A probabilistic model predictive control approach. Math. Biosci. Eng. **19**(9), 8804–8832 (2022)

39. Moore, S., Hill, E.M., Tildesley, M.J., et al.: Vaccination and non-pharmaceutical interventions for COVID-19: a mathematical modelling study. Lancet Infect. Dis. **21**(6), 793–802 (2021)
40. Laine, M.: Adaptive MCMC methods with applications in environmental and geophysical models. PhD thesis, Lappeenranta University of Technology, Lappeenranta, Finland (2008)

Publisher's Note

Springer Nature remains neutral with regard to jurisdictional claims in published maps and institutional affiliations.